Epithelial Ablation of Bcl-X_L Increases Sensitivity to Oxygen without Disrupting Lung Development

Rhonda J. Staversky[1], Peter F. Vitiello[1], Min Yee[1], Linda M. Callahan[2], David A. Dean[1], and Michael A. O'Reilly[1]

[1]Department of Pediatrics, and [2]Department of Pathology and Laboratory Medicine, School of Medicine and Dentistry, University of Rochester, Rochester, New York

Recent studies indicate that the antiapoptotic Bcl-X_L, one of five isoforms expressed by the *Bcl-X* gene, protects a variety of cell lines exposed to hyperoxia. However, its role in lung development and protection against oxidative stress *in vivo* is not known. Here, we show Bcl-X_L is the predominant isoform expressed in the lung, and the only isoform detected in respiratory epithelium. Because loss of Bcl-X_L is embryonically lethal, Bcl-X_L was ablated throughout the respiratory epithelium by mating mice with a floxed exon II of the *Bcl-X* gene with mice expressing Cre under control of the surfactant protein-C promoter. Interestingly, the loss of Bcl-X_L in respiratory epithelium was perinatally lethal in approximately 50% of the expected offspring. However, some adult mice lacking the gene were obtained. The epithelial-specific ablation of Bcl-X_L did not disrupt pulmonary function, the expression of epithelial cell–specific markers, or lung development. However, it shifted the lung toward a proapoptotic state, defined by a reduction in antiapoptotic Mcl-1, an increase in proapoptotic Bak, and increased sensitivity of the respiratory epithelium to hyperoxia. Intriguingly, increased 8-oxoguanine lesions seen during hyperoxia were also evident as lungs transitioned to room air at birth, a time when perinatal lethality in some mice lacking Bcl-X_L was observed. These findings reveal that the epithelial-specific expression of Bcl-X_L is not required for proper lung development, but functions to protect respiratory epithelial cells against oxygen-induced toxicity, such as during hyperoxia and the lung's first exposure to ambient air.

Keywords: apoptosis; development; oxidative stress

CLINICAL RELEVANCE

Mechanisms by which the respiratory epithelium defends against oxidative stress, such as the stress caused by increasing oxygen tensions, are not fully defined. We reveal that antiapoptotic protein Bcl-X_L protects the respiratory epithelium against the oxidative stress caused by oxygen, but is not essential for proper lung development.

The primary function of the lung, and in particular respiratory epithelial cells, is to deliver and exchange oxidant gases effectively between the environment and blood. At the same time, the lung must protect itself against both external and intrinsic agents that provoke cell injury and death. Extrinsic agents include air pollution and proinflammatory cytokines such as TNF-α or FasL, whereas intrinsic agents include intracellular reactive oxygen species (ROS) and signals emanating from damaged DNA or unfolded proteins. Airway and alveolar epithelial cells are further challenged by ROS produced by their continuous exposure to ambient air (1). These oxygen-induced ROS are likely to be elevated rapidly at birth when the lung is first exposed to oxygen, or when elevated oxygen (hyperoxia) is used to treat respiratory distress (2). The fate of oxidized cells is dictated by the production of antioxidant defense molecules, repair pathways, and genes that control survival and death. Given that antioxidant defenses are only partially efficacious against oxidative lung injury (3), a better understanding of the genes involved in determining the fate of injured cells is needed.

Cell survival and death are controlled by members of the *Bcl-2* gene family, now numbering more than 20, that share homology in one to four regions designated as *Bcl-2* homology (BH) domains, as reviewed elsewhere (4). The multidomain members can be subdivided into two groups, based on their ability to promote survival (Bcl-2, Bcl-X_L, Bcl-w, Bfl-1/A1, and Mcl-1) or cell death (Bax and Bak). The single BH3-only members (Bad, Bid, Bim, Noxa, PUMA, HRK, BMF, and NBK/BIK) become activated in response to extrinsic and intrinsic death stimuli, such as damaged DNA. Recent studies suggest that a subset of these single-domain proteins binds antideath Bcl-2 proteins, thereby releasing a second subset of single BH-3 proteins that activate Bax-dependent and Bak-dependent cell death (5, 6). Consistent with hyperoxia inducing cell death via this family, fibroblasts derived from $Bax^{-/-}$ $Bak^{-/-}$ mice exhibit increased resistance to hyperoxia (7). On the other hand, the overexpression of antideath Bcl-X_L, Mcl-1, Bfl-1/A1, or Bcl-2 in cell lines or mice protects against hyperoxia (7–10). Although less is known about the role of the single BH3-only proteins during hyperoxia, caspase 8 activation and Bid cleavage in response to the Fas-induced death signaling complex were reported in A549 human lung carcinoma cells (11). Although this suggests that hyperoxia activates extrinsic death stimuli, our studies indicate that hyperoxia also activates intrinsic death signaling via the ATM-p53 DNA damage pathway (12, 13). In turn, P53 stimulates the expression of cyclin-dependent kinase inhibitor p21 and the prodeath Bcl-2 protein Puma (14). During hyperoxia, P21 antagonizes prodeath signals by delaying the loss of Bcl-X_L and Mcl-1, and Bcl-X_L specifically blocks Bax-dependent cell death (10, 15).

Despite this strong evidence for the involvement of Bcl-2–related proteins during hyperoxia, their role in specific cell types in the lung remains undefined. The lung is composed of more than 40 cell types, and among these, hyperoxia largely promotes the death of alveolar microvascular endothelial and type I epithelial cells (16). Mechanisms underlying this cell-restricted sensitivity to hyperoxia remain to be clarified, and in fact may be caused by the selective expression or activation of prodeath and antideath members of the Bcl-2 family. We previously reported that hyperoxia stimulates the mRNA for Bcl-X_L and Bax in bronchiolar epithelial and alveolar cells of adult mice (17). Although hyperoxia stimulated Bcl-X_L protein in that

(*Received in original form May 11, 2009 and in final form October 21, 2009*)

This study was supported in part by National Institutes of Health grants HL-67392 and HL-091968 (M.A.O.) and HL-81148 and HL-59956 (D.A.D.), and by March of Dimes grant 6-FY08–264 (M.A.O.). The animal inhalation facility was supported by National Institutes of Health Center Grant ES-01247.

Correspondence and requests for reprints should be addressed to Michael A. O'Reilly, Ph.D., Department of Pediatrics, School of Medicine and Dentistry, University of Rochester, 601 Elmwood Avenue, Box 850, Rochester, NY 14642. E-mail: michael_oreilly@urmc.rochester.edu

Am J Respir Cell Mol Biol Vol 43. pp 376–385, 2010
Originally Published in Press as DOI: 10.1165/rcmb.2009-0165OC on October 30, 2009
Internet address: www.atsjournals.org

study, we subsequently discovered that the antibody does not recognize Bcl-X_L, and in fact, Bcl-X_L protein declines during hyperoxia (15). The *Bcl-X* gene encodes both prodeath and antideath isoforms generated by the alternative splicing of mRNAs transcribed from multiple promoters (18–20). The most common isoform is Bcl-X_L, and it is encoded by exons II and III. Bcl-X_S contains an internal deletion of Bcl-X_L, and Bcl-$X_{\Delta TM}$ undergoes alternative splicing that produces a frame-shift and translation termination, 8 base pairs (bp) after the stop codon in Bcl-X_L. Bcl-X_β is encoded by an unspliced variant of exon II, and Bcl-Xγ is encoded by exon II splicing to novel exons IV, V, and VI. Thus, all isoforms except Bcl-X_S share a common 188 amino-acid amino-terminal domain, with small differences in the carboxy terminus. *In vitro* translation and overexpression of individual isoforms revealed that Bcl-X_L, Bcl-$X_{\Delta TM}$, and Bcl-Xγ are antiapoptotic, whereas Bcl-X_S and Bcl-X_β are proapoptotic. Five promoters located with 3.5 kb of exon II are thought to influence alternative splicing, and hence the expression of these various Bcl-X isoforms (21).

The complexity of the *Bcl-X* gene, and the lack of antibodies specific for individual isoforms, make it challenging to understand how the *Bcl-X* gene controls the survival of individual cells in a heterocellular organ such as the lung. This is especially problematic when loss of the *Bcl-X* gene causes early embryonic lethality, attributed to massive apoptosis of immature erythroid progenitors in fetal liver (22). Tissue-specific ablation was achieved in a variety of tissues, using specific Cre drivers that ablate the first two exons (23–25). Here, we used surfactant protein-C (Sftpc)–Cre driver mice to investigate how selective loss of the *Bcl-X* locus throughout the respiratory epithelium affects lung development and the response to hyperoxia-induced lung injury. Some of the findings were presented as a poster at the American Thoracic Society Meeting of May 2009.

MATERIALS AND METHODS

Mice

Mice were housed in sterile microisolator cages in a specified pathogen-free environment, with approval of the Committee on Animal Resources at the University of Rochester. The Sftpc–Cre mice (strain C57Bl6/J) were mated to floxed *Bcl-X* (strain Swiss Webster from Lothar Hennighausen at NIH, Bethesda, MD) or floxed mT/mG (Jackson Laboratories, Bar Harbor, ME) mice. Heterozygous F1-generation *Bcl-X* mice were backcrossed to obtain F2 progeny, whereas the heterozygous F1-generation of mT/mG mice was sacrificed for study. To genotype mice, tail biopsies were digested at 55°C in lysis buffer including proteinase K (1 μg/ml) (26). Genomic DNA was precipitated in 100% isopropanol, washed in 70% ethanol, and resuspended in buffer containing 10 mM Tris and 1 mM EDTA, pH 8.0. The Bcl-X wild-type and floxed genotypes were amplified from 100 ng genomic DNA, using forward primer (5′-CGGTTGCCTAGCAACGGGGC-3′) and reverse primer (5′-CTCCCACAGTGGAGACCTCG-3′), with 30 cycles at 94°C, 58°C, and 72°C each for 30 seconds (24). The Cre genotype was amplified with forward (5′-TTCGGCTATACGTAACAGGG-3′) and reverse (5′-TCGATGCAACGAGTGATGAG-3′) primers, using 30 cycles of 94°C for 30 seconds, 55°C for 30 seconds, and 72°C for 1 minute. The amplified Bcl-X wild-type (200 bp), Bcl-X floxed (300 bp), and Cre (500 bp) products were detected by agarose gel electrophoresis.

Lung Mechanics

At 8 weeks of age, five mice were anesthetized with sodium pentobarbital (40 mg/kg). The trachea was exposed and connected to a computer-controlled, small animal mechanical ventilator (flexiVent; SCIREQ, Montreal, PQ, Canada), as previously described (27). Mice were injected intraperitoneally with pancuronium (1 mg/kg) to paralyze the diaphragm, and mice were ventilated with 8 ml/kg at a rate of 150 breaths/minute, with a positive end-expiratory pressure of 2 cm H_2O. Estimated tissue damping and tissue elastance were obtained from the flexiVent by fitting a model to each impedance spectrum (28).

RNA Isolation and RT-PCR

Lungs were homogenized in 4 M guanidine isothiocyanate, 0.5% *N*-laurylsarcosine, 20 mM sodium citrate, and 0.1 M 2-mercaptoethanol. The RNA was extracted using acid phenol and phase-lock columns (5 Prime-3Prime, Boulder, CO), and resuspended in diethylpyrocarbonate (DEPC)-treated water. type II cells were isolated as described elsewhere (29) and lysed in Trizol reagent (Invitrogen, Carlsbad, CA). The RNA was precipitated in isopropanol and resuspended in DEPC-treated water. Complementary DNA was prepared using an iScript cDNA Synthesis kit (Bio-Rad, Hercules, CA) at 25°C for 5 minutes, 42°C for 30 minutes, 85°C for 5 minutes, and 4°C for 5 minutes. The *Bcl-X* isoforms were amplified using 5′ forward primer GATC GAATTCATGTCTCAGAGCAACCGGGA. The reverse primers used were GATCAGATCTTCATTTCCGACTGAAGAGTG for Bcl-X_L and Bcl-X_S, GATCAGATCTTGCATGTAGTGGTTCTCCTC for Bcl-$X_{\Delta TM}$, GATCAGATCTAAGATACAGGTCCCTTAA for Bcl-X_β, and GATCAGATCTCGTCCTTCCTGAAGTCCTCC for Bcl-Xγ. Complementary DNAs were amplified at 95°C, 60°C, and 72°C each for 30 seconds for 35 cycles. We detected Bcl-X_L (701 bp), Bcl-X_S (512 bp), Bcl-$X_{\Delta TM}$ (731 bp), Bcl-X_β (772 bp), and Bcl-X_γ (979 bp) isoforms, using agarose gel electrophoresis. Primer sequences and amplification conditions for surfactant protein C (SP-C), Type I alpha (T1α), Clara cell secretory protein (CCSP), and platelet endothelial cell adhesion molecule (PECAM) were described previously (30).

Lung Histology and Staining

The left lobes were tied off, and the right lobes were inflation-fixed through the trachea for 10 minutes with 10% neutral-buffered formalin at 20 cm pressure. The fixed lobe was dehydrated in graded alcohol and embedded in paraffin. Tissue sections (5 μm) were deparaffinized in Pro-Par clearant (Anatech, Ltd., Battle Creek, MI) and rehydrated through a series of ethanol to water. Lung sections were then stained with hematoxylin and eosin. To detect Bcl-X protein, sections were boiled in 10 mM citrate buffer, pH 6, followed by a hydrogen peroxide block, PBS wash, and avidin/biotin block (catalogue number SP-2001; Vector

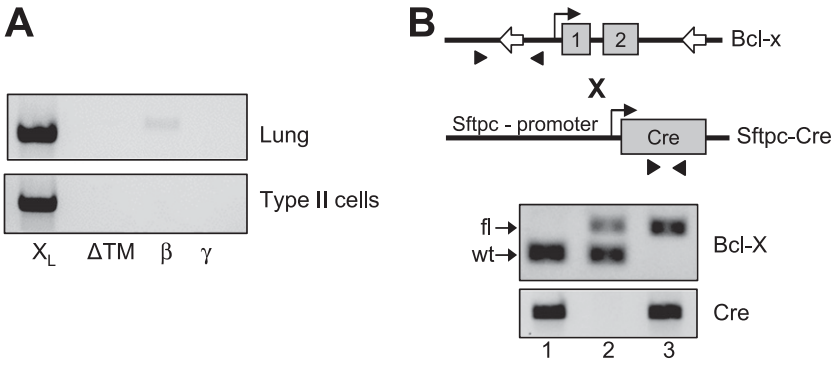

Figure 1. Genotypic analysis of Sftpc–Cre and floxed *Bcl-X* mice. (*A*) Representative RT-PCR analysis of *Bcl-X* isoforms detected in whole-lung RNA or type II cell RNA. (*B*) Depiction of floxed *Bcl-X* and *Sftpc–Cre* genes, with primers (*arrowheads*) used for genotyping mice. *Open arrows* in *Bcl-X* gene represent LoxP site flanking exons 1 and 2. Below the cartoon is a representative PCR analysis of genomic tail DNA, showing wild-type (*wt*) and floxed (*fl*) products of the *Bcl-X* and *Cre* genes.

TABLE 1. PREDICTED AND ACTUAL GENOTYPIC FREQUENCIES OF F_2 OFFSPRING BETWEEN Sftpc–Cre AND FLOXED *Bcl-X* MATINGS

Genotype of F_2 Mice	*Bcl-X* in Lung Epithelium	Predicted Frequency (%)	Adult Frequency (%)	Embryonic Frequency (%)
Cre^{-}:*Bcl-X*$^{wt/wt}$	Homozygous	6.25	37.50	10.00
Cre^{+}:*Bcl-X*$^{wt/wt}$	Homozygous	18.75	23.21	40.00
Cre^{-}:*Bcl-X*$^{wt/fl}$	Homozygous	12.50	8.93	6.67
Cre^{-}:*Bcl-X*$^{fl/fl}$	Homozygous	6.25	11.61	6.67
Cre^{+}:*Bcl-X*$^{wt/fl}$	Heterozygous	37.50	11.61	3.33
Cre^{+}:*Bcl-X*$^{fl/fl}$	Knockout	18.75	7.14	33.33

Mice were genotyped by PCR, using primers that detect the wild-type and floxed alleles of *Bcl-X*, and the *Cre* gene. Adult frequencies were determined from 112 mice (52 males and 60 females) at 21 days of age, and embryonic frequencies were determined from 30 mice on Embryonic Day 18.

Laboratories, Burlingame, CA). Sections were then blocked with a Mouse on Mouse kit (catalogue number PK-2200; Vector Laboratories, Inc.), followed by incubation overnight with mouse anti-Bcl-X antibody (catalogue number B9429; Sigma, St. Louis, MO). Immune complexes were detected with biotinylated mouse antibody, and visualized as brown precipitate, using 3,3′-diaminobenzidine (Vectastain Elite; Vector Laboratories). Stained slides were counterstained with hematoxylin (Zymed, South San Francisco, CA) and visualized with a Nikon E800 microscope (Nikon, Melville, NY) coupled to a SPOT-RT digital camera (Diagnostic Instruments, Sterling Heights, MI). For visualizing *Discosoma sp.* red (DsRed) and enhanced green fluorescence protein (EGFP) in mT/mG transgenic mice, rehydrated tissues were immunostained with anti-EGFP antibody and counterstained with DAPI (31). Images were captured on an Olympus FV1000 laser scanning confocal microscope with Fluoview version 2.0 software (Olympus America, Center Valley, PA), using sequential scanning and adjusting only the photomultiplier tube voltage. Copies of images were postprocessed for brightness and contrast only, using FV1000 postprocessing features.

Western Blots

Lung tissues were homogenized with a polytron in 1 ml lysis buffer (15). Proteins were separated by size, using a polyacrylamide gel, and transferred to polyvinylidene fluoride membrane. Membranes were blocked in 5% dried milk in Tris-buffered saline + 0.1% Tween-20, and immunoblotted with primary antibody for 1 hour at room temperature (anti-actin, catalogue number A2066; Sigma) or overnight at 4°C (anti–Bcl-X, catalogue number B9429; Sigma; anti–Mcl-1, catalogue number 32087; Abcam, Cambridge, MA; anti-Bcl-2, catalogue number BD554279; BD Pharmingen, San Diego CA; anti-Bak, catalogue number AM03; Calbiochem, Gibbstown, NJ; anti-Bax, catalogue number SC-493; Santa Cruz Biotechnology, Santa Cruz, CA; anti–proSP-C, catalogue number AB3786; Chemicon, Temecula, CA; anti-CCSP was provided by Barry

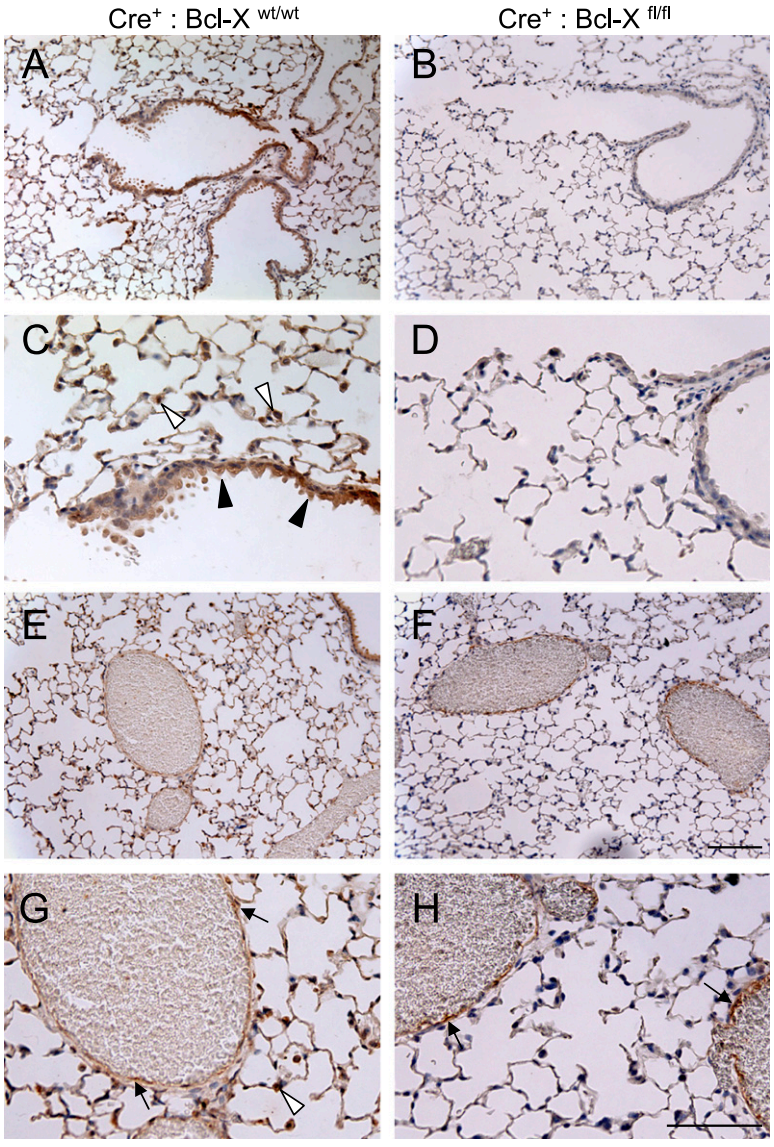

Figure 2. Immunohistochemical staining of Bcl-X protein in *Bcl-X* control and knockout mice. Lungs from Cre^{+}:*Bcl-X*$^{wt/wt}$ (*A*, *C*, *E*, and *G*) and Cre^{+}:*Bcl-X*$^{fl/fl}$ (*B*, *D*, *F*, and *H*) mice were immunostained for Bcl-X protein that was detected as a brown stain, using 3,3′-diaminobenzidine. Sections were lightly counterstained with hematoxylin. *Solid arrowheads* denote airway epithelium, *open arrowheads* denote alveolar epithelium, and *arrows* denote vascular endothelium. *Inset bar* in *F* = 100 μm, and in *H* = 50 μm.

Stripp at Duke University; T1-α was provided by the Iowa Hybridoma Bank; and anti-PECAM, catalogue number SC1506; Santa Cruz). Blots were washed in PBS–Tween and incubated with horseradish peroxidase–conjugated secondary antibodies, and proteins were detected by chemiluminescence (ECL kit; GE Lifesciences, Piscataway, NJ), using blue-sensitive film (Laboratory Products Sales, Rochester, NY). Band intensities were visualized on a gel documentation system (Alpha Innotech, San Leandro, CA), and quantified using Image J software.

Measurements of Hyperoxia and Lung Injury

Mice were exposed to room air or 100% oxygen (hyperoxia) that was humidified to 40–70% by passing through deionized water-jacketed Nafion membrane tubing (PermPure, LLC, Toms River, NJ). Animals were lavaged four times with 1 ml sterile saline. Samples from an individual mouse were pooled, and cells were removed by centrifugation. The supernatant was assayed for protein concentrations, using a BCA protein assay kit (Thermo Scientific, Rockford, IL). The left lobe was fixed, sectioned, and stained with an apoptosis detection kit (catalogue number S7165; Serologicals Corp., Norcross, GA), using fluorescent antibodies or FITC-labeled 8-oxoguanine–binding peptide (31). The 8-oxoguanine–positive cells were quantified using MetaMorph software (Molecular Devices, Sunnyvale, CA) according to the thresholded area of FITC compared with DAPI. Terminal deoxynucleotidyl transferase dUTP nick end labeling (TUNEL)-positive and DAPI-positive cells were quantified using Metaview software (Molecular Devices).

Statistical Analysis

Values are expressed as means ± standard deviations. Group means were compared according to ANOVA, using Fisher *post hoc* analysis with Statview software (Abacus Concepts, Inc., Berkeley, CA). $P < 0.05$ was considered significant.

RESULTS

Epithelial Ablation of Bcl-X Does Not Disrupt Lung Function or Development in Adult Mice

The Bcl-X locus encodes five alternatively spliced isoforms that differ in their carboxy terminus (18–20). Because isoform-specific antibodies are not available, the expression of individual isoforms was investigated by RT-PCR, using a common 5′ primer and isoform-specific 3′ primers for Bcl-X_L, Bcl-X_S, Bcl-$X_{\Delta TM}$, Bcl-X_β, and Bcl-X_γ. We readily detected Bcl-X_L in whole lung, and Bcl-X_β was faintly detected (Figure 1A). We did not detect Bcl-X_S, Bcl- $X_{\Delta TM}$, and Bcl-X_γ. Although Bcl-X_L and Bcl-X_β were detected in whole lung, only Bcl-X_L was detected in freshly isolated preparations of type II epithelial cells. Using primers specific for type II cells (SP-C), TYPE I cells (T1α), airway (CCSP), and endothelium (PECAM), RT-PCR confirmed that our isolated cell preparations were predominantly type II, with some contaminating airway Clara cells (data not shown). These findings indicate that antiapoptotic Bcl-X_L is the predominant isoform of the *Bcl-X* gene expressed by respiratory epithelium and the lung in general.

The floxed *Bcl-X* gene contains a single loxP site in the 5′-flanking region and a second loxP site in the second intron, thereby allowing ablation of the proximal promoter region and exons 1 and 2 (Figure 1B) (23). Because exon 2 encodes all five isoforms of *Bcl-X*, this targeting strategy ablates both proapoptotic and antiapoptotic members of the *Bcl-X* gene. To ablate *Bcl-X* throughout the respiratory epithelium, the floxed *Bcl-X* mice were mated to Sftpc–Cre transgenic mice (32). The F_1-generation mice were screened for the presence of the *Cre* gene, because all mice were heterozygous for the floxed Bcl-X allele. The Sftpc–Cre–positive mice were then mated to each other to obtain F_2 mice, with or without the *Cre* transgene and wild-type or floxed forms of the *Bcl-X* gene (Table 1). Although the expected numbers of Cre^+:$Bcl\text{-}X^{wt/wt}$ mice were obtained, significantly more Cre^-:$Bcl\text{-}X^{wt/wt}$ were obtained than expected, suggesting that the presence of Cre recombinase with a floxed Bcl-X allele was lethal. Indeed, only 50% of the predicted mice containing Cre^+ and both floxed alleles of *Bcl-X* ($Bcl\text{-}X^{fl/fl}$) were detected, and they were identified in both male and female mice. Surprisingly, only 30% of the expected numbers of Cre^+ and heterozygous *Bcl-X* ($Bcl\text{-}X^{wt/fl}$)

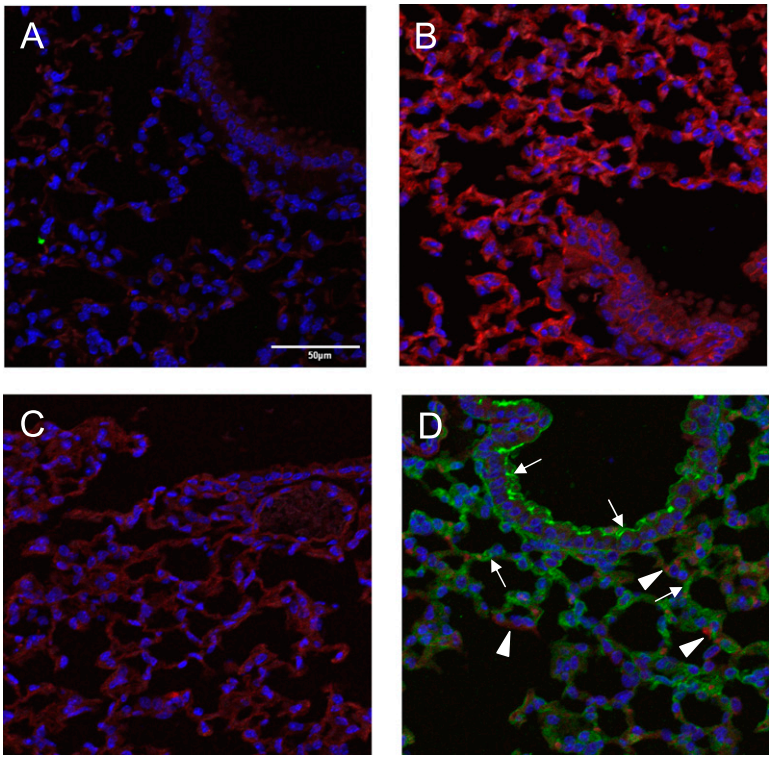

Figure 3. Epithelial-specific recombination of mT/mG mice, using Sftpc–Cre mice. Lungs from *Sftpc–Cre* (*A*), $mT/mG^{+/+}$ (*B*), Cre^- $mT/mG^{+/-}$ (*C*), and Cre^+ $mT/mG^{+/-}$ (*D*) mice were stained for EGFP and DAPI. Fluorescent images for intrinsic red from the membrane targeted *tdTomato* gene, FITC-stained EGFP, and DAPI were obtained using confocal microscopy. *Arrows* indicate respiratory epithelial cells expressing EGFP, and *arrowheads* indicate nonrespiratory epithelial cells expressing the *tdTomato* gene. *Bar* in *A* = 50 μm.

mice were obtained. To determine whether mice were being lost at birth, mice were genotyped on embryonic day 18. Consistent with increased perinatal lethality, *Cre*$^{+}$:*Bcl-X*$^{fl/fl}$ mice were readily identified on embryonic day 18. Intriguingly, the number of positive embryos was higher than expected, perhaps because the number of *Cre*$^{+}$:*Bcl-X*$^{wt/fl}$ was lower than predicted, but that finding might be attributed to the relatively low number of embryos screened ($n = 30$). The pathology of E18.5 *Cre*$^{+}$:*Bcl-X*$^{fl/fl}$ appeared normal and indistinguishable from control animals ($n = 10$; data not shown). The few surviving *Cre*$^{+}$:*Bcl-X*$^{fl/fl}$ mice were then mated to each other to establish a line of conditionally knocked out mice. However, for unknown reasons, only one of five mating pairs produced progeny, and this only happened once. This outcome suggested that *Cre*$^{+}$:*Bcl-X*$^{fl/fl}$ mice were not sterile, but for unknown reasons, displayed reduced fecundity. Despite our best efforts to rotate the mating pairs and modify their housing conditions, a conditional line of mice lacking *Bcl-X* could not be established, and so the present study was performed with mice derived from F_1 crosses.

Using an antibody against the amino terminus, and thus recognizing all isoforms, Bcl-X_L protein was readily detected in airway epithelial cells and alveolar cells in corners consistent with type II epithelial cells of *Cre*$^{+}$:*Bcl-X*$^{wt/wt}$ control mice (Figures 2A and 2C). It was also detected in endothelial cells of large veins, but not in thin alveolar walls composed of microvascular endothelial cells and type I epithelial cells (Figures 2E and 2G). Similar patterns of expression were seen with other genotypes (data not shown). However, Bcl-X_L protein was not observed in airway and alveolar type II cells of *Cre*$^{+}$:*Bcl-X*$^{fl/fl}$ mice (Figures 2B and 2D). It was detected in large veins, which is consistent with the Sftpc promoter selectively targeting Cre recombinase to the respiratory epithelium and not other cell types (Figures 2E and 2H).

Two approaches were used to confirm the epithelial restricted ablation of Bcl-X_L, using Sftpc–Cre. First, Sftpc–Cre mice were mated to homozygous mT/mG mice, which contain a floxed membrane-targeted tdTomato (mT) cassette, followed by membrane-targeted EGFP (mG) under the control of cytomegalovirus enhancer/chicken β-actin core promoter (33). In the presence of Cre recombinase, the ubiquitous expression of mT (a variant of DsRed) is replaced by EGFP. As expected, intrinsic and ubiquitous red-shifted fluorescence was observed throughout the lungs of homozygous mT/mG mice, but not Sftpc–Cre mice (Figure 3). When mated to each other, F1 progeny were heterozygous for the mT/mG locus, which led to an overall reduction in intrinsic red fluorescence. Although EGFP was not detected in Cre-negative mice, the early developmental expression of Sftpc in the lung resulted in a near ubiquitous activation of green fluorescence throughout the respiratory epithelium in the Cre-positive offspring.

Western blot analysis of whole-lung homogenates was also used to confirm that Bcl-X protein was significantly reduced to 22% ± 1.7% in *Cre*$^{+}$:*Bcl-X*$^{fl/fl}$ lungs, compared with control *Cre*$^{+}$:*Bcl-X*$^{wt/wt}$ lungs (Figure 4A; $P = 0.017$). Based on its size of 28 kD, the knowledge that Bcl-X_L comprises 234 amino acids and Bcl-X_β comprises 210 amino acids, and the knowledge that Bcl-X_L mRNA is the predominant isoform in the lung and the respiratory epithelium, the detected Bcl-X protein is likely to be Bcl-X_L. Surprisingly, loss of Bcl-X_L led to a significant reduction to 19% ± 4.3% in the expression of antiapoptotic Mcl-1 ($P = 0.0013$), but not Bcl-2 ($P = 0.93$) (Figure 4A). It also led to an increase (2.1 ± 0.02-fold) in the expression of proapoptotic Bak ($P = 0.018$), but not Bax ($P = 0.88$). These findings suggest that a loss of Bcl-X_L shifts the respiratory epithelium to a proapoptotic state.

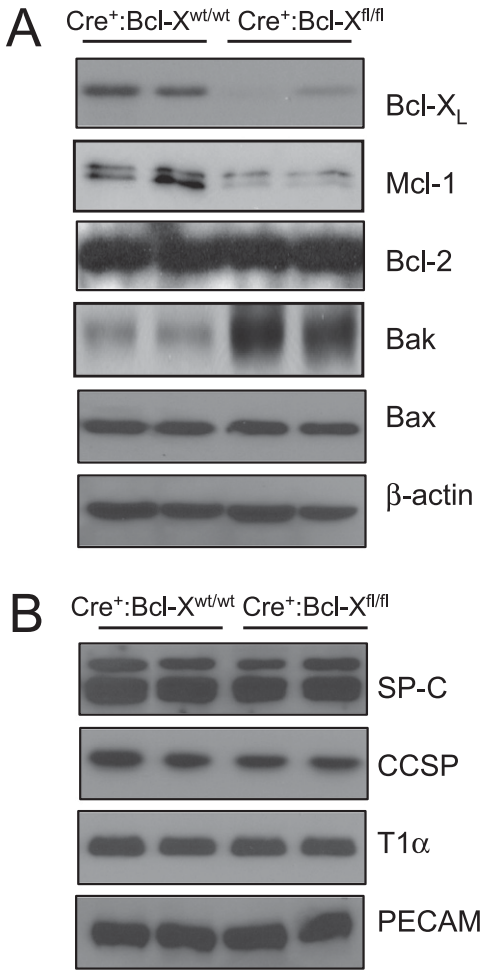

Figure 4. Gene expression in control and *Bcl-X* conditional knockout mice. (*A*) Lungs from *Cre*$^{+}$:*Bcl-X*$^{wt/wt}$ and *Cre*$^{+}$:*Bcl-X*$^{fl/fl}$ mice were immunoblotted for Bcl-X_L, Mc-1, Bcl-2, Bak, Bax, and actin. (*B*) Lungs from *Cre*$^{+}$:*Bcl-X*$^{wt/wt}$ and *Cre*$^{+}$:*Bcl-X*$^{fl/fl}$ mice were immunoblotted for proSP-C, CCSP, T1α, and PECAM. Each lane represents a different mouse, and blots are representative of five mice for each group.

Despite the partial perinatal loss of *Cre*$^{+}$:*Bcl-X*$^{fl/fl}$ mice and the loss of Bcl-X_L in the respiratory epithelium, lung histology in mice that survived to adulthood appeared normal (Figure 2). Loss of the *Bcl-X* gene did not alter the expression of proteins expressed by type II cells (proSP-C; $P = 0.88$), airway Clara cells (Clara cell secretory protein; $P = 0.64$), type I cells (T1α; $P = 0.81$), and endothelial cells (PECAM or CD31; $P = 0.77$) (Figure 4B). It also did not affect airway resistance ($P = 0.75$), airway elastance ($P = 0.98$), alveolar compliance ($P = 0.43$), tissue damping ($P = 0.97$), or tissue elastance ($P = 0.77$), as measured on a flexiVent (Figure 5). These findings indicate that epithelial loss of the *Bcl-X* gene is perinatally lethal in some mice, but those that survive to adulthood present with normal lung structure and function.

Epithelial Ablation of the *Bcl-X* Gene Increases Sensitivity of Respiratory Epithelium to Oxygen

Although type I epithelial cells are sensitive to hyperoxia, the relative resistance of airway and alveolar type II cells may be attributed in part to their expression of Bcl-X_L. To test this, TUNEL staining was performed on lungs harvested from *Cre*$^{+}$:*Bcl-X*$^{wt/wt}$ and *Cre*$^{+}$:*Bcl-X*$^{fl/fl}$ mice that were exposed to room air or 100% oxygen for 60 hours. Less than 1% of lung

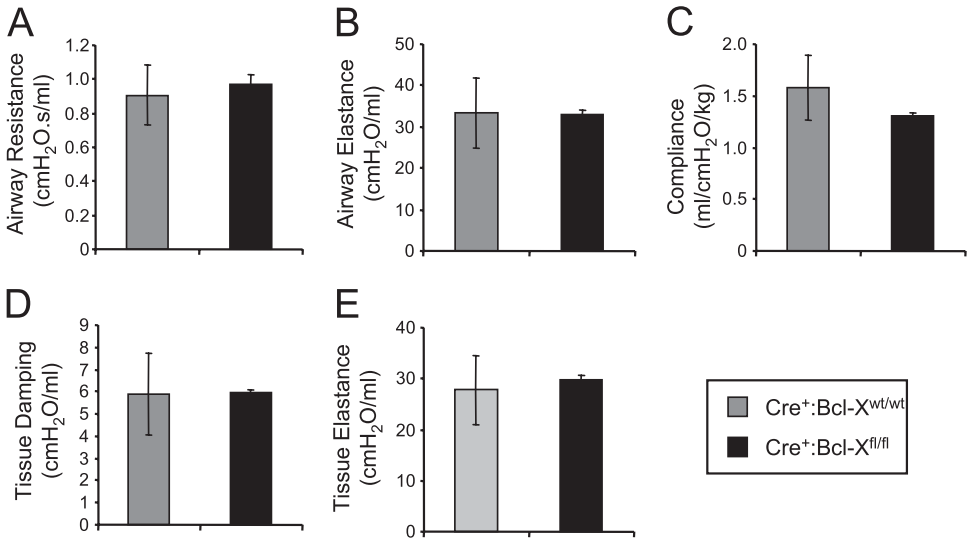

Figure 5. Lung mechanics in control and *Bcl-X* conditional knockout mice. Airway resistance (*A*), airway elastance (*B*), alveolar compliance (*C*), tissue damping (*D*), and tissue elastance (*E*) were measured in *Cre*$^+$:*Bcl-X*$^{wt/wt}$ and *Cre*$^+$:*Bcl-X*$^{fl/fl}$ mice. Values represent mean ± SD of four control mice (*Cre*$^+$:*Bcl-X*$^{wt/wt}$) and three knockout mice (*Cre*$^+$:*Bcl-X*$^{fl/fl}$) per group.

cells from control mice exposed to room air were TUNEL-positive, and this amount was unaffected by the loss of Bcl-X_L (Figure 6). We detected TUNEL-positive staining in 3.4 ± 0.76 cells of *Cre*$^+$:*Bcl-X*$^{wt/wt}$ mice exposed to hyperoxia, compared with 8.7% ± 4% of *Cre*$^+$:*Bcl-X*$^{fl/fl}$ mice ($n = 5$ per group; $P < 0.02$), as largely observed in distal airway and alveoli (Figure 7A). Although hyperoxia increased alveolar-capillary membrane permeability, as defined by protein in bronchoalveolar lavage fluid ($P < 0.0001$), it was not significantly different in mice lacking the *Bcl-X* gene that were also exposed to hyperoxia (Figure 7B). This observation confirms the specificity of the Sftpc promoter to drive Cre and hence ablate the Bcl-X locus selectively in the respiratory epithelium and not other cell types.

To investigate oxidant DNA damage further, lungs were immunostained for 8-oxoguanine. As previously reported (31, 34), 3.0% ± 0.22% of airway and alveolar epithelial cells of adult *Cre*$^+$:*Bcl-X*$^{wt/wt}$ mice exposed to room air had detectable 8-oxoguanine staining, and this markedly increased to 29.9% ± 1.0% ($P < 0.0001$) in mice exposed to hyperoxia (Figures 8A and 8B). Similarly, 8-oxoguanine staining was evident in 1.2% ± 0.5% of *Cre*$^+$:*Bcl-X*$^{fl/fl}$ mice exposed to room air, and this increased to 19.9% ± 2.5% ($P < 0.0001$) in mice exposed to

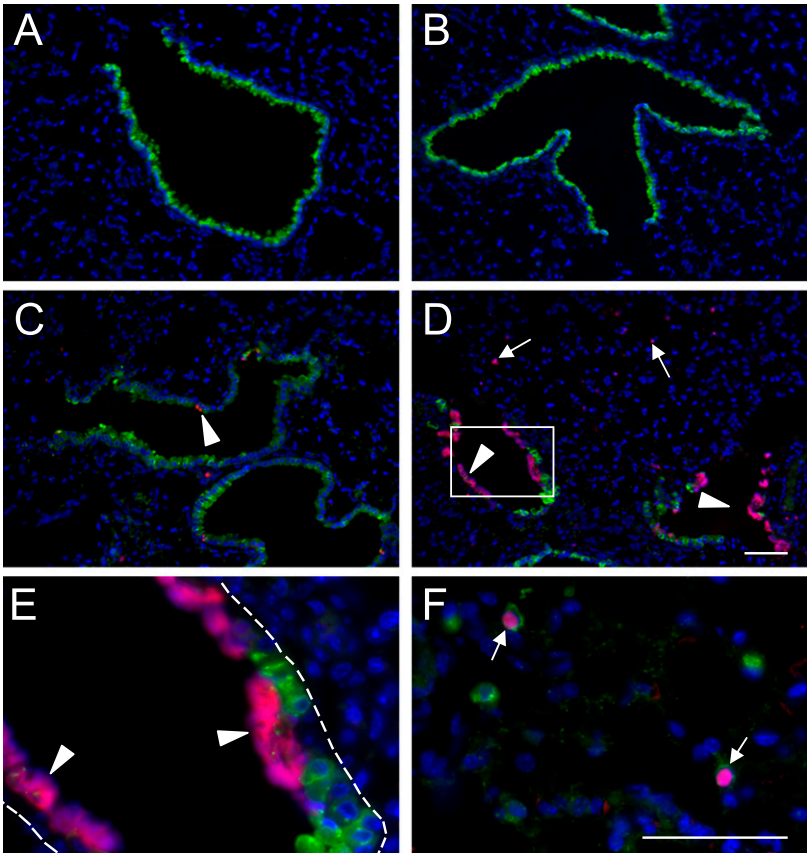

Figure 6. Apoptosis in control and *Bcl-X* conditional knockout mice exposed to hyperoxia. *Cre*$^+$:*Bcl-X*$^{wt/wt}$ (control) and *Cre*$^+$:*Bcl-X*$^{fl/fl}$ (knockout) conditional knockout mice were exposed to room air or hyperoxia for 60 hours. Representative images are of TUNEL staining in control and floxed *Bcl-X* mice exposed to room air (*A, B*) or hyperoxia (*C, D*) for 60 hours. Lungs of *Cre*$^+$:*Bcl-X*$^{fl/fl}$ mice exposed to hyperoxia were stained for TUNEL (*red*) and CCSP (*E*) or proSP-C (*F*) (*green*). *Arrowheads* indicate TUNEL-positive cells in airway and *arrows* indicate TUNEL-positive cells in alveoli. *Dotted line* in *E* defines the basement membrane of the airway. *Inset bar* = 50 μm.

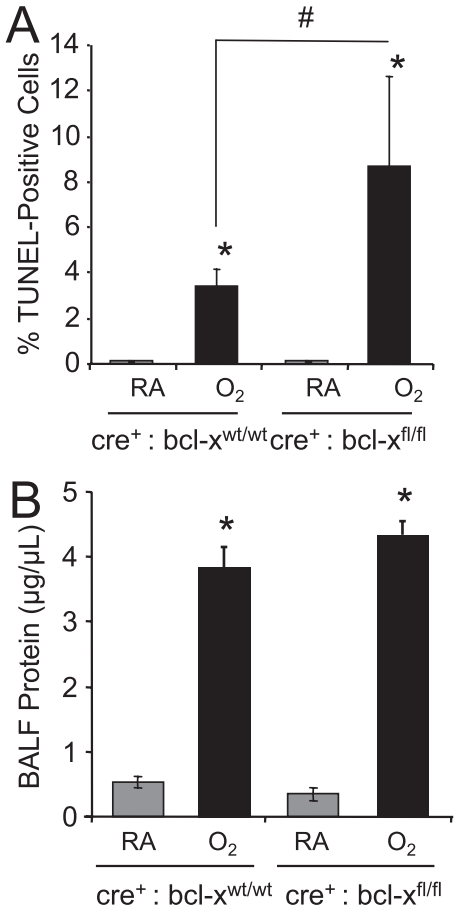

Figure 7. Apoptosis and edema in control and *Bcl-X* conditional knockout mice exposed to hyperoxia. (*A*) The number of TUNEL-positive cells to total number of DAPI-positive cells in Cre^{+}:$Bcl\text{-}X^{wt/wt}$ and Cre^{+}:$Bcl\text{-}X^{fl/fl}$ mice exposed to room air or hyperoxia was graphed. Values represent mean ± SD for $n = 5$ mice per group (*$P < 0.0001$ and $^{\#}P = 0.02$) (*B*) Total protein in bronchoalveolar lavage fluid of Cre^{+}:$Bcl\text{-}X^{wt/wt}$ and Cre^{+}:$Bcl\text{-}X^{fl/fl}$ mice exposed to room air or hyperoxia was quantified and graphed. Values represent mean ± SD for $n = 5$ mice per group (*$P < 0.0001$).

hyperoxia (data not shown). Although loss of Bcl-X_L did not affect the percentage of 8-oxoguanine–positive cells in mice exposed to room air, it did reduce the number of positive cells seen in mice exposed to hyperoxia ($P < 0.0001$). However, this result could be an underestimation, because the significant epithelial injury seen in hyperoxic Cre^{+}:$Bcl\text{-}X^{fl/fl}$ mice reduced the DAPI staining (a fluorescent dye that intercalates in double-stranded DNA) used to identify individual cells. Nonetheless, the perinatal loss of some mice lacking Bcl-X_L led us to speculate that oxidized lesions are produced at birth, when the lung is exposed to ambient air. To test this, lungs were harvested on Embryonic Day 18.5 and Postnatal Days 0.5, 2, and 14, and stained for 8-oxoguanine, using adult lungs as control samples. Intriguingly, 8-oxoguanine–positive cells were not detected in Embryonic Day 18.5 lungs (Figures 8C and 8E). Although staining was not evident on Postnatal Day 0.5 (data not shown), 8-oxoguanine–positive cells were readily detected in 7.2% ± 0.7% of the distal respiratory epithelium on Postnatal Day 2 (Figures 8D and 8F). Higher-power magnification revealed that the staining was both nuclear and cytoplasmic. The cytoplasmic staining was punctate and consistent with the mitochondrial localization previously reported in adult mice exposed to hyperoxia (31). Staining was slightly decreased by Postnatal Day 14 (data not shown), but still greater than that seen in 8-week adult mice, implying that repair may be occurring.

DISCUSSION

Respiratory epithelial cells are constantly under oxidative stress caused by exposure to molecular oxygen and inhaled oxidizing pollutants. Despite strong evidence that Bcl-X_L, an antiapoptotic protein encoded by the *Bcl-X* gene, protects cultured cell lines against hyperoxia-induced cell death, its role in proper lung development and protection against oxidative stress *in vivo* is not known. Here we provide evidence Bcl-X_L is the predominant isoform expressed in the lung, and confirm through Cre-mediated recombination that it functions to protect the respiratory epithelium *in vivo* against hyperoxia-induced cell death. Although loss of Bcl-X_L did not noticeably disrupt lung function or development, perinatal lethality was observed in some mice, leading us to consider that Bcl-X_L may protect against the oxidative damage caused by exposure to ambient air at birth. Indeed, exposure to room air at birth oxidizes DNA, much like the exposure of adults to hyperoxia. Our findings confirm that Bcl-X_L protects the respiratory epithelium against hyperoxia, and provide new evidence that it may serve to protect against oxidative damage created as the lung transitions to ambient air at birth.

The *Bcl-X* gene encodes multiple isoforms created by alternative splicing of RNA transcripts generated from multiple promoters (21). Whereas Bcl-X_S, Bcl-X_β, and Bcl-Xγ promote apoptosis, Bcl-X_L and Bcl-$X_{\Delta TM}$ possess antiapoptotic activities. Although it remains unclear how promoter choice and alternative splicing control the expression of individual isoforms, they are required for the proper development of some tissues. For instance, germline ablation of the *Bcl-X* gene causes massive apoptosis of postmitotic neurons of the brain, spinal cord, and dorsal root ganglion (22). Shortened lifespans of immature lymphocytes are also seen, and the mice die by Embryonic Day 13. Erythroid-specific ablation using mouse mammary tumor virus-long terminal repeat/Cre driver mice causes the hyperproliferation of megakaryocytes and immature erythroid cells, and hemolytic anemia by age 3 months (24). These deficits could be rescued by simultaneously ablating Bax. The conditional deletion of *Bcl-X* in mammary epithelium caused accelerated apoptosis of the epithelium during involution, but increased apoptosis could not be reduced by deleting Bax (25). The inability to rescue mammary gland development by deleting Bax implies that erythroid and mammary cells express different isoforms of the *Bcl-X* gene, or that Bcl-X_L acts to block Bax in some cell types and not in others. Regardless, we found that normal lung development and function was unaffected by ablation of the *Bcl-X* gene in the respiratory epithelium. Because Bcl-X_L was the only isoform detected in respiratory epithelium, this suggests that apoptosis (e.g., the low levels of apoptosis seen in postnatal rats) may not be absolutely required for specifying proper lung development and function (35). Alternatively, the apoptosis of epithelial cells is important for lung maturation, but the process does not involve Bcl-X_L.

On the other hand, loss of Bcl-X_L increases the sensitivity of respiratory epithelium to hyperoxia, as defined according to TUNEL staining and histologic features of cell necrosis. Because biotin was not used to amplify staining, the number of TUNEL-positive cells reported here was much lower than in previous studies (31, 34, 36). Because TUNEL staining during hyperoxia is associated with oxygen-induced DNA strand breaks, the omission of biotin allowed us to identify those cells with the most severe DNA damage as they died (31). The increased number of TUNEL-positive but not 8-oxoguanine–

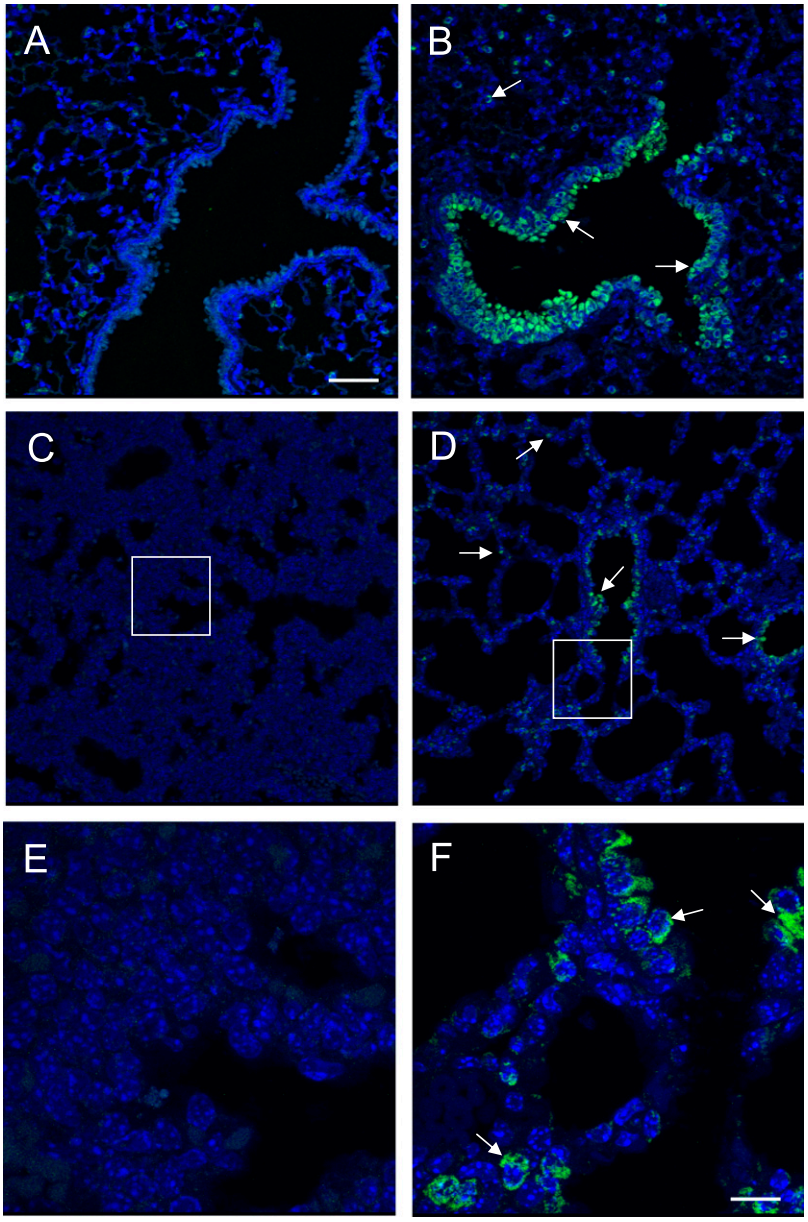

Figure 8. Oxygen promotes 8-oxoguanine lesions in the lung. Lungs of adult mice exposed to room air (*A*) and lungs of adult mice exposed to hyperoxia (*B*) on Embryonic Day 18.5 (*C*, *E*), and Postnatal Day 2 (*D*, *F*) were stained with FITC-labeled 8-oxoguanine–binding peptide. Sections were counterstained with DAPI, and images were captured by confocal microscopy. *Inset box* in *C* and *D* is magnified 3-fold in *E* and *F*. *Arrows* indicate 8-oxoguanine–positive cells. *Bar* = 50 μm for *A–D*, and 10 μm for *E* and *F*.

positive cells in hyperoxic mice lacking Bcl-X_L suggests that Bcl-X_L protects against signals coming from DNA damage (e.g., p53, Puma, Noxa, or Bak) that promote cell death and hence the degradation of DNA (37–39). Our findings in mice lacking Bcl-X_L confirm studies in mouse-lung epithelial MLE12 cells, Rat1a fibroblasts, and *p21*-deficient HCT116 colon carcinoma cells, showing that the overexpression of Bcl-X_L protects against hyperoxia-induced Bax activation and cell death (7, 14, 40). The overexpression of Bcl-X_L does not protect A549 human lung adenocarcinoma cells against hyperoxia (11). However, this is because A549 cells express the cell-cycle–inhibitor p21, which delays the loss of Bcl-X_L during exposure (10, 41). Unlike findings in *p21*-deficient mice exposed to hyperoxia (42), increased alveolar–capillary membrane permeability and mortality were not evident in mice lacking the epithelial expression of Bcl-X_L. This finding implies that alveolar–capillary membrane permeability, at least for this length of exposure, is not affected by injury to the respiratory epithelium. This is consistent with histologic observations that microvascular endothelial cells are more sensitive to hyperoxia, and their loss leads to increased vascular permeability and mortality (43–45).

Although Bcl-X_L is not required for proper lung development, our study suggests that it protects the developing lung from oxidative damage as it becomes exposed to ambient air at birth. This is a critical period during which the lung undergoes oxidative stress as it transitions from a relatively hypoxic *in utero* to an oxygen-rich *ex utero* environment. Although oxidative damage attributed to exposure to room air at birth has not been extensively studied, plasma levels of F2-isoprostanes are high in early human infants, and decline by 6 months of age (46). The elevated expression of antioxidant defense enzymes, as reported in newborn rats, is thought to protect against such oxidative stress (47, 48). Consistent with this idea, the targeted overexpression of manganese-superoxide dismutase or extracellular-superoxide dismutase to the respiratory epithelium protects the developing lung against hyperoxia (49, 50). However, mice lacking these enzymes are normal, implying a redundancy in antioxidant defense mechanisms required for adaptation of the lung to oxygen (3). However, the present

study indicates that these antioxidant defense mechanisms are insufficient to block oxidative stress fully, because increased 8-oxoguanine lesions were evident in newborn mice. Instead, antiapoptotic proteins such as Bcl-X_L appear to provide an additional line of defense by blocking apoptotic signals emanating from oxidized molecules such as DNA. Interestingly, 8-oxoguanine staining was both nuclear and cytoplasmic, because cytoplasmic staining was seen in newborn rats and adult mice exposed to hyperoxia (31, 51). This may reflect the oxidation of mitochondrial DNA, because 8-oxoguanine staining in mice colocalized to cytochrome-C oxidase subunit 1. Intriguingly, mitochondrial dysfunction was recently associated with arrested lung development in newborn mice exposed to hyperoxia, and Bcl-X_L functioned to maintain mitochondrial homeostasis (52, 53). Although levels of Bcl-X_L were similar in newborn and adult mice (data not shown), targeting additional levels to developing lungs exposed to hyperoxia may provide a novel therapy for preventing BPD.

The loss of Bcl-X_L by itself shifted the lung toward a proapoptotic state, as defined by a reduction in antiapoptotic Mcl-1 and an increase in proapoptotic Bak. These were selective changes, because the expression of Bcl-2 and Bax were unaffected. How the loss of Bcl-X_L affected the expression of Mcl-1 and Bak is unclear. Studies on the effects of germline or Cre-mediated ablation of Bcl-X_L in other tissues did not investigate how loss of Bcl-X_L affected the expression of other members of the Bcl-2 family (22–25). The silencing RNA knockdown of Bcl-X_L in cell lines (A549, H1299, and HCT116) does not affect the expression of Mcl-1 or Bak (unpublished observations). On the other hand, similar changes in expression of these Bcl-2–related proteins were seen when these cell lines were exposed to hyperoxia (10, 11, 14, 41). This implies that the Bcl-2 rheostat of the respiratory epithelium was shifted in *Cre* $^{+}$:*Bcl-X*$^{fl/fl}$ mice as if they were already in a state of hyperoxia. Viewed this way, it may be less surprising to find that they are hypersensitive to hyperoxia or even oxygen exposure at birth. Although additional studies are needed to understand how Bcl-X_L maintains the expression of Mcl-1 and Bak, Bcl-X_L should be considered equivalent in importance to antioxidants for defending the respiratory epithelium against oxidative damage created by inhaled pollutants or oxygen at birth.

A limitation of this study was our inability to generate a line of mice lacking epithelial *Bcl-X*, and we have no explanation for this failure. The Sftpc–Cre and unfloxed *Bcl-X* lines of mice breed in a normal Mendelian manner, and produced the expected F1 progeny when bred together. Although viable F2 mice were obtained, we were unsuccessful at generating a line of mice using five independent mating pairs. One pair produced F3 progeny, but only once, and pregnancy was never observed in the other pairs. Thus, the present study was largely performed on a limited number of F2 mice obtained from F1 heterozygote matings. A remote but possible explanation is that Cre expression is "leaky" in the germline. Indeed, as these studies were nearing completion, we learned that some germline leakiness was observed (personal communication with Barry Stripp at Duke University). Although it remains to be determined whether that was responsible for our failure to create a line of mice, enough mice were created for us to conclude that Bcl-X_L protects respiratory epithelial cells against oxidative damage when oxygen tensions increase, but is not required for proper lung development.

Author Disclosure: M.A.O. received a sponsored research grant from the National Institutes of Health (NIH) for more than $100,001 and from the March of Dimes for $50,001–$100,000. R.J.S. received a sponsored research grant from the NIH for more than $100,001. M.Y. received a sponsored research grant from the NIH for more than $100,001 and from the March of Dimes for $50,001–$100,000. D.A.D. received a sponsored grant from the NIH for more than $100,001, and his spouse/life partner received a sponsored grant from the American Heart Association for more than $100,001. None of the other authors has a financial relationship with a commercial entity that has an interest in the subject of this manuscript.

Acknowledgments: The authors thank Brigid Hogan for providing the Sftpc–Cre mice and Lothar Hennighausen for providing the floxed *Bcl-X* mice. The authors also thank Emma Rawlins for providing primer sequences and conditions for genotyping Sftpc–Cre mice.

References

1. Fridovich I. Oxygen toxicity: a radical explanation. *J Exp Biol* 1998;201: 1203–1209.
2. Jenkinson SG. Oxygen toxicity. *New Horiz* 1993;1:504–511.
3. Ho YS. Transgenic and knockout models for studying the role of lung antioxidant enzymes in defense against hyperoxia. *Am J Respir Crit Care Med* 2002;166:S51–S56.
4. Danial NN, Korsmeyer SJ. Cell death: critical control points. *Cell* 2004; 116:205–219.
5. Kim H, Rafiuddin-Shah M, Tu HC, Jeffers JR, Zambetti GP, Hsieh JJ, Cheng EH. Hierarchical regulation of mitochondrion-dependent apoptosis by Bcl-2 subfamilies. *Nat Cell Biol* 2006;8:1348–1358.
6. Willis SN, Fletcher JI, Kaufmann T, van Delft MF, Chen L, Czabotar PE, Ierino H, Lee EF, Fairlie WD, Bouillet P, *et al.* Apoptosis initiated when bh3 ligands engage multiple Bcl-2 homologs, not Bax or Bak. *Science* 2007;315:856–859.
7. Budinger GR, Tso M, McClintock DS, Dean DA, Sznajder JI, Chandel NS. Hyperoxia-induced apoptosis does not require mitochondrial reactive oxygen species and is regulated by Bcl-2 proteins. *J Biol Chem* 2002;277:15654–15660.
8. He CH, Waxman AB, Lee CG, Link H, Rabach ME, Ma B, Chen Q, Zhu Z, Zhong M, Nakayama K, *et al.* Bcl-2–related protein A1 is an endogenous and cytokine-stimulated mediator of cytoprotection in hyperoxic acute lung injury. *J Clin Invest* 2005;115:1039–1048.
9. Metrailler-Ruchonnet I, Pagano A, Carnesecchi S, Ody C, Donati Y, Barazzone Argiroffo C. Bcl-2 protects against hyperoxia-induced apoptosis through inhibition of the mitochondria-dependent pathway. *Free Radic Biol Med* 2007;42:1062–1074.
10. Vitiello PF, Wu YC, Staversky RJ, O'Reilly MA. P21(CIP1) protects against oxidative stress by suppressing ER-dependent activation of mitochondrial death pathways. *Free Radic Biol Med* 2009;46:33–41.
11. Wang X, Ryter SW, Dai C, Tang ZL, Watkins SC, Yin XM, Song R, Choi AM. Necrotic cell death in response to oxidant stress involves the activation of the apoptogenic caspase-8/BID pathway. *J Biol Chem* 2003;278:29184–29191.
12. Gehen SC, Staversky RJ, Bambara RA, Keng PC, O'Reilly MA. HSMG-1 and ATM sequentially and independently regulate the G(1) checkpoint during oxidative stress. *Oncogene* 2008;27:4065–4074.
13. Helt CE, Cliby WA, Keng PC, Bambara RA, O'Reilly MA. Ataxia telangiectasia mutated (ATM) and ATM and RAD3-related protein exhibit selective target specificities in response to different forms of DNA damage. *J Biol Chem* 2005;280:1186–1192.
14. Vitiello PF, Staversky RJ, Keng PC, O'Reilly MA. Puma inactivation protects against oxidative stress through p21/Bcl-X_L inhibition of Bax death. *Free Radic Biol Med* 2008;44:367–374.
15. Vitiello PF, Staversky RJ, Gehen SC, Johnston CJ, Finkelstein JN, Wright TW, O'Reilly MA. P21CIP1 protection against hyperoxia requires Bcl-X_L and is uncoupled from its ability to suppress growth. *Am J Pathol* 2006;168:1838–1847.
16. Crapo JD, Barry BE, Foscue HA, Shelburne J. Structural and biochemical changes in rat lungs occurring during exposures to lethal and adaptive doses of oxygen. *Am Rev Respir Dis* 1980;122:123–143.
17. O'Reilly MA, Staversky RJ, Huyck HL, Watkins RH, LoMonaco MB, D'Angio CT, Baggs RB, Maniscalco WM, Pryhuber GS. Bcl-2 family gene expression during severe hyperoxia induced lung injury. *Lab Invest* 2000;80:1845–1854.
18. Shiraiwa N, Inohara N, Okada S, Yuzaki M, Shoji S, Ohta S. An additional form of rat Bcl-X, Bcl-Xbeta, generated by an unspliced RNA, promotes apoptosis in promyeloid cells. *J Biol Chem* 1996;271: 13258–13265.
19. Boise LH, Gonzalez-Garcia M, Postema CE, Ding L, Lindsten T, Turka LA, Mao X, Nunez G, Thompson CB. *Bcl-x*, a Bcl-2-related gene that functions as a dominant regulator of apoptotic cell death. *Cell* 1993; 74:597–608.

20. Yang XF, Weber GF, Cantor H. A novel Bcl-X isoform connected to the T cell receptor regulates apoptosis in T cells. *Immunity* 1997;7:629–639.
21. Pecci A, Viegas LR, Baranao JL, Beato M. Promoter choice influences alternative splicing and determines the balance of isoforms expressed from the mouse *Bcl-X* gene. *J Biol Chem* 2001;276:21062–21069.
22. Motoyama N, Wang F, Roth KA, Sawa H, Nakayama K, Negishi I, Senju S, Zhang Q, Fujii S, Loh DY. Massive cell death of immature hematopoietic cells and neurons in *Bcl-X*–deficient mice. *Science* 1995;267:1506–1510.
23. Rucker EB III, Dierisseau P, Wagner KU, Garrett L, Wynshaw-Boris A, Flaws JA, Hennighausen L. *Bcl-X* and Bax regulate mouse primordial germ cell survival and apoptosis during embryogenesis. *Mol Endocrinol* 2000;14:1038–1052.
24. Wagner KU, Claudio E, Rucker EB III, Riedlinger G, Broussard C, Schwartzberg PL, Siebenlist U, Hennighausen L. Conditional deletion of the *Bcl-X* gene from erythroid cells results in hemolytic anemia and profound splenomegaly. *Development* 2000;127:4949–4958.
25. Walton KD, Wagner KU, Rucker EB III, Shillingford JM, Miyoshi K, Hennighausen L. Conditional deletion of the *Bcl-X* gene from mouse mammary epithelium results in accelerated apoptosis during involution but does not compromise cell function during lactation. *Mech Dev* 2001;109:281–293.
26. Laird PW, Zijderveld A, Linders K, Rudnicki MA, Jaenisch R, Berns A. Simplified mammalian DNA isolation procedure. *Nucleic Acids Res* 1991;19:4293.
27. Mutlu GM, Machado-Aranda D, Norton JE, Bellmeyer A, Urich D, Zhou R, Dean DA. Electroporation-mediated gene transfer of the Na+,K+–ATPase rescues endotoxin-induced lung injury. *Am J Respir Crit Care Med* 2007;176:582–590.
28. Ito S, Lutchen KR, Suki B. Effects of heterogeneities on the partitioning of airway and tissue properties in normal mice. *J Appl Physiol* 2007; 102:859–869.
29. Rice WR, Conkright JJ, Na CL, Ikegami M, Shannon JM, Weaver TE. Maintenance of the mouse type II cell phenotype in vitro. *Am J Physiol Lung Cell Mol Physiol* 2002;283:L256–L264.
30. Roper JM, Staversky RJ, Finkelstein JN, Keng PC, O'Reilly MA. Identification and isolation of mouse type II cells based upon intrinsic expression of enhanced green fluorescent protein. *Am J Physiol Lung Cell Mol Physiol* 2003;285:L691–L700.
31. Roper JM, Mazzatti DJ, Watkins RH, Maniscalco WM, Keng PC, O'Reilly MA. *In vivo* exposure to hyperoxia induces DNA damage in a population of alveolar type II epithelial cells. *Am J Physiol Lung Cell Mol Physiol* 2004;286:L1045–L1054.
32. Okubo T, Knoepfler PS, Eisenman RN, Hogan BL. NMYC plays an essential role during lung development as a dosage-sensitive regulator of progenitor cell proliferation and differentiation. *Development* 2005;132:1363–1374.
33. Muzumdar MD, Tasic B, Miyamichi K, Li L, Luo L. A global double-fluorescent Cre reporter mouse. *Genesis* 2007;45:593–605.
34. Barker GF, Manzo ND, Cotich KL, Shone RK, Waxman AB. DNA damage induced by hyperoxia: quantitation and correlation with lung injury. *Am J Respir Cell Mol Biol* 2006;35:277–288.
35. Schittny JC, Djonov V, Fine A, Burri PH. Programmed cell death contributes to postnatal lung development. *Am J Respir Cell Mol Biol* 1998;18:786–793.
36. Buckley S, Barsky L, Driscoll B, Weinberg K, Anderson KD, Warburton D. Apoptosis and DNA damage in type 2 alveolar epithelial cells cultured from hyperoxic rats. *Am J Physiol* 1998;274:L714–L720.
37. Nakano K, Vousden KH. *Puma*, a novel proapoptotic gene, is induced by p53. *Mol Cell* 2001;7:683–694.
38. Shibue T, Takeda K, Oda E, Tanaka H, Murasawa H, Takaoka A, Morishita Y, Akira S, Taniguchi T, Tanaka N. Integral role of NOXA in p53-mediated apoptotic response. *Genes Dev* 2003;17: 2233–2238.
39. Yu J, Zhang L, Hwang PM, Kinzler KW, Vogelstein B. *Puma* induces the rapid apoptosis of colorectal cancer cells. *Mol Cell* 2001;7:673–682.
40. Buccellato LJ, Tso M, Akinci OI, Chandel NS, Budinger GR. Reactive oxygen species are required for hyperoxia-induced Bax activation and cell death in alveolar epithelial cells. *J Biol Chem* 2004;279:6753–6760.
41. Staversky RJ, Vitiello PF, Gehen SC, Helt CE, Rahman A, Keng PC, O'Reilly MA. P21(CIP1/WAF1/SDI1) protects against hyperoxia by maintaining expression of Bcl-X(L). *Free Radic Biol Med* 2006;41: 601–609.
42. O'Reilly MA, Staversky RJ, Watkins RH, Reed CK, de Mesy Jensen KL, Finkelstein JN, Keng PC. The cyclin-dependent kinase inhibitor p21 protects the lung from oxidative stress. *Am J Respir Cell Mol Biol* 2001;24:703–710.
43. Adamson IY, Bowden DH, Wyatt JP. Oxygen poisoning in mice. Ultrastructural and surfactant studies during exposure and recovery. *Arch Pathol* 1970;90:463–472.
44. Bowden DH, Adamson IY, Wyatt JP. Reaction of the lung cells to a high concentration of oxygen. *Arch Pathol* 1968;86:671–675.
45. Kapanci Y, Weibel ER, Kaplan HP, Robinson FR. Pathogenesis and reversibility of the pulmonary lesions of oxygen toxicity in monkeys. II. Ultrastructural and morphometric studies. *Lab Invest* 1969; 20:101–118.
46. Friel JK, Friesen RW, Harding SV, Roberts LJ. Evidence of oxidative stress in full-term healthy infants. *Pediatr Res* 2004;56:878–882.
47. Clerch LB, Massaro D. Rat lung antioxidant enzymes: differences in perinatal gene expression and regulation. *Am J Physiol* 1992;263: L466–L470.
48. Chen Y, Frank L. Differential gene expression of antioxidant enzymes in the perinatal rat lung. *Pediatr Res* 1993;34:27–31.
49. Ahmed MN, Suliman HB, Folz RJ, Nozik-Grayck E, Golson ML, Mason SN, Auten RL. Extracellular superoxide dismutase protects lung development in hyperoxia-exposed newborn mice. *Am J Respir Crit Care Med* 2003;167:400–405.
50. Wispe JR, Warner BB, Clark JC, Dey CR, Neuman J, Glasser SW, Crapo JD, Chang LY, Whitsett JA. Human Mn-superoxide dismutase in pulmonary epithelial cells of transgenic mice confers protection from oxygen injury. *J Biol Chem* 1992;267:23937–23941.
51. Auten RL, Whorton MH, Nicholas Mason S. Blocking neutrophil influx reduces DNA damage in hyperoxia-exposed newborn rat lung. *Am J Respir Cell Mol Biol* 2002;26:391–397.
52. Ratner V, Starkov A, Matsiukevich D, Polin RA, Ten VS. Mitochondrial dysfunction contributes to alveolar developmental arrest in hyperoxia-exposed mice. *Am J Respir Cell Mol Biol* 2009;40:511–518.
53. Vander Heiden MG, Chandel NS, Williamson EK, Schumacker PT, Thompson CB. Bcl-X_L regulates the membrane potential and volume homeostasis of mitochondria. *Cell* 1997;91:627–637.